AD-A120 861 ELECTRON AND PROTON SPECTROMETRY IN THE AFGL AURORAL E 1/1
PROGRAM I EXPERIME..(U) AIR FORCE GEOPHYSICS LAB
HANSCOM AFB MA W J MCMAHON ET AL. 09 APR 82
UNCLASSIFIED AFGL-TR-82-0121 FFG 7/4 NL

END

MICROCOPY RESOLUTION TEST CHART
NATIONAL BUREAU OF STANDARDS-1963-A

MICROCOPY RESOLUTION TEST CHART
NATIONAL BUREAU OF STANDARDS-1963-A

MICROCOPY RESOLUTION TEST CHART
NATIONAL BUREAU OF STANDARDS-1963-A

MICROCOPY RESOLUTION TEST CHART
NATIONAL BUREAU OF STANDARDS-1963-A

MICROCOPY RESOLUTION TEST CHART
NATIONAL BUREAU OF STANDARDS-1963-A

AFGL-TR-82-0121
ENVIRONMENTAL RESEARCH PAPERS, NO. 776

Electron and Proton Spectrometry in the AFGL Auroral E Program I. Experiment Overview and Preliminary Auroral Electron Data

W. J. McMAHON
L. HEROUX
R. H. SALTER

9 April 1982

AERONOMY DIVISION PROJECT 6690
AIR FORCE GEOPHYSICS LABORATORY
HANSCOM AFB, MASSACHUSETTS 01731

AIR FORCE SYSTEMS COMMAND, USAF

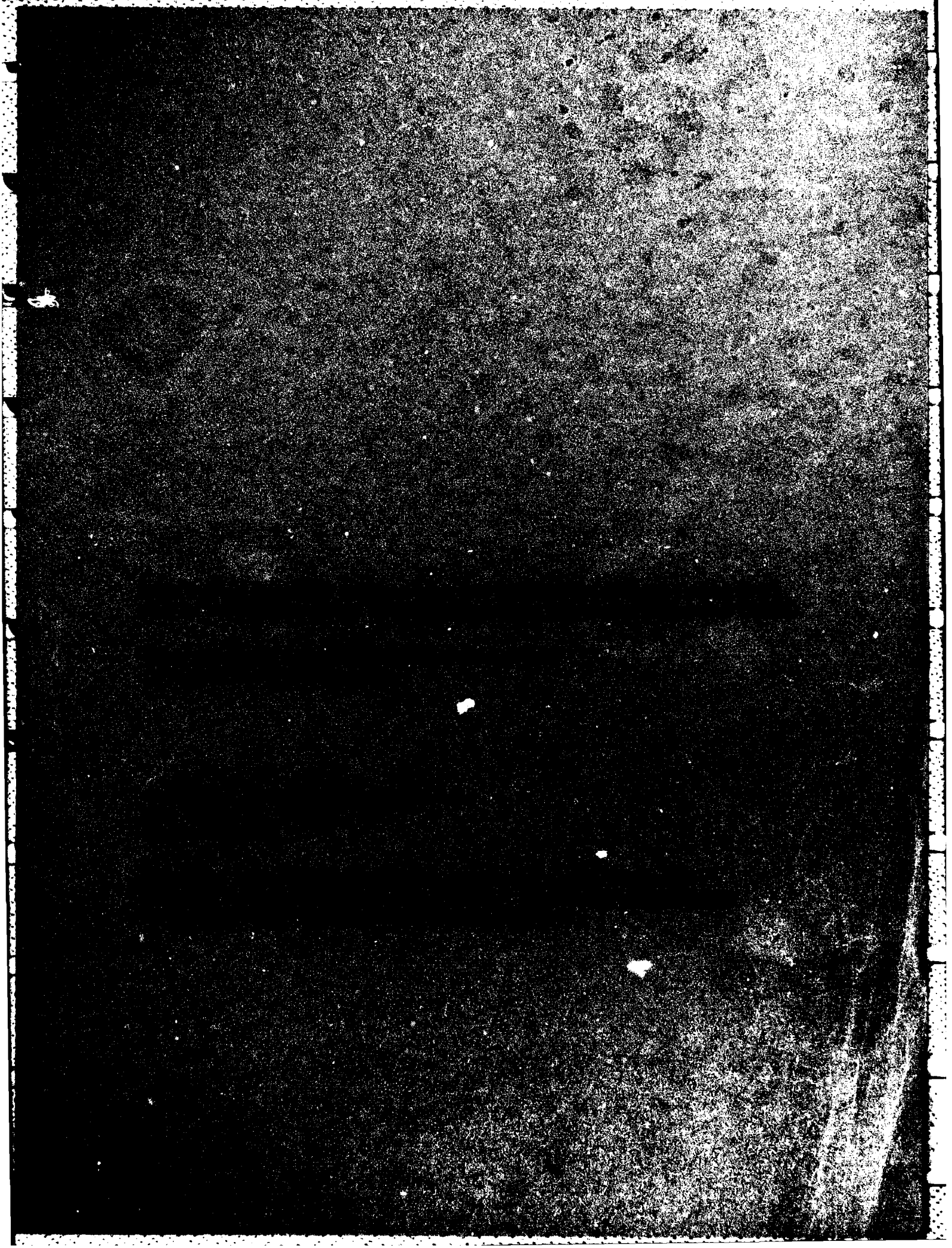

AFGL-TR-82-0121
9 APRIL 1982
ENVIRONMENTAL RESEARCH PAPERS, NO. 776

ELECTRON AND PROTON SPECTROMETRY IN THE AFGL AURORAL E PROGRAM I. EXPERIMENT OVERVIEW AND PRELIMINARY AURORAL ELECTRON DATA

W.J. McMahon
L. Heroux
R.H. Salter

ERRATA

On page 5, the title of the report should read:

Electron and Proton Spectrometry in the
AFGL Auroral E Program
I. Experiment Overview and Preliminary
Auroral Electron Data

AIR FORCE GEOPHYSICS LABORATORY
AIR FORCE SYSTEMS COMMAND
UNITED STATES AIR FORCE
HANSCOM AFB, MASSACHUSETTS 01731

Unclassified

SECURITY CLASSIFICATION OF THIS PAGE (When Data Entered)

REPORT DOCUMENTATION PAGE		READ INSTRUCTIONS BEFORE COMPLETING FORM
1. REPORT NUMBER AFGL-TR-82-0121	2. GOVT ACCESSION NO. AD-A120861	3. RECIPIENT'S CATALOG NUMBER
4. TITLE (and Subtitle) ELECTRON AND PROTON SPECTROMETRY IN THE AFGL AURORAL E PROGRAM. I. EXPERIMENT OVERVIEW AND PRELIMINARY AURORAL ELECTRON DATA		5. TYPE OF REPORT & PERIOD COVERED Scientific. Interim. 6. PERFORMING ORG. REPORT NUMBER ERP. No. 776
7. AUTHOR(s) W. J. McMahon L. Heroux R. H. Salter		8. CONTRACT OR GRANT NUMBER(s)
9. PERFORMING ORGANIZATION NAME AND ADDRESS Air Force Geophysics Laboratory (LKO) Hanscom AFB Massachusetts 01731		10. PROGRAM ELEMENT, PROJECT, TASK AREA & WORK UNIT NUMBERS 62101F 66901606
11. CONTROLLING OFFICE NAME AND ADDRESS Air Force Geophysics Laboratory (LKO) Hanscom AFB Massachusetts 01731		12. REPORT DATE 9 April 1982 13. NUMBER OF PAGES 23
14. MONITORING AGENCY NAME & ADDRESS(if different from Controlling Office)		15. SECURITY CLASS. (of this report) Unclassified 15a. DECLASSIFICATION/DOWNGRADING SCHEDULE

16. DISTRIBUTION STATEMENT (of this Report)

Approved for public release; distribution unlimited

17. DISTRIBUTION STATEMENT (of the abstract entered in Block 20, if different from Report)

18. SUPPLEMENTARY NOTES

19. KEY WORDS (Continue on reverse side if necessary and identify by block number)

Electron spectrometry
Auroral electrons
Ionospheric electron flux
Electron energy distribution

20. ABSTRACT (Continue on reverse side if necessary and identify by block number)

The design of spectrometers to determine electron and proton spectra over energy ranges between 2 eV and 60 keV, and their application in a dual rocket experiment to measure these particle fluxes in a continuous aurora, are discussed briefly. Details of the overall experiment, including relevant flight parameters, are given, and preliminary results of electron measurements are presented.

DD FORM 1 JAN 73 1473 EDITION OF 1 NOV 65 IS OBSOLETE

Unclassified

SECURITY CLASSIFICATION OF THIS PAGE (When Data Entered)

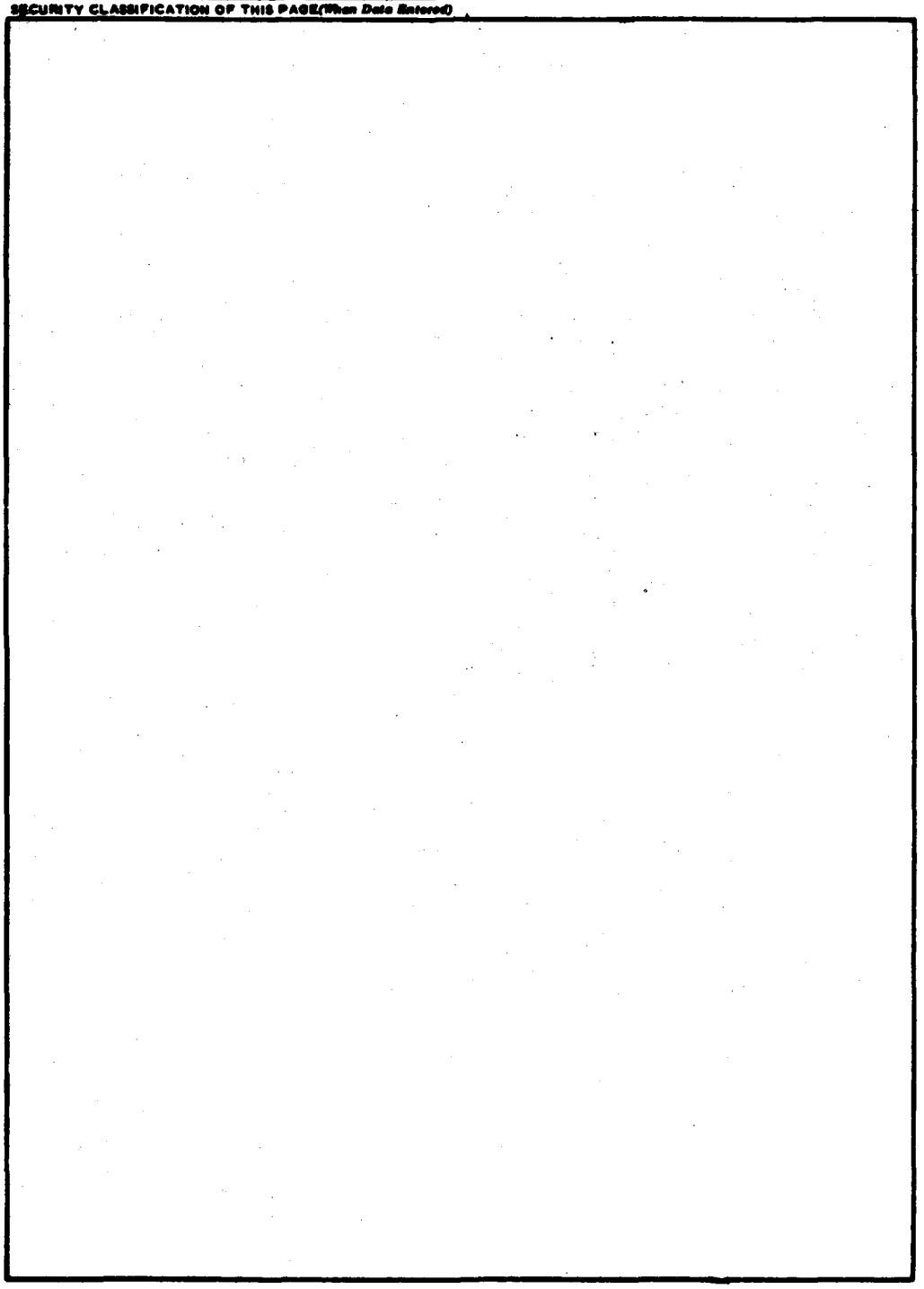

Contents

Illustrations

Illustrations

Tables

Electron and Proton Spectrometry in the AFGL Auroral E Program I. Experiment Overview and Preliminary Electron Data

1. INTRODUCTION

One of the experimental objectives of the AFGL Auroral E Program was the in situ determination of electron and proton spectra in the continuous (diffuse) aurora. To achieve this objective, it was necessary to design rocket-borne spectrometers to measure the energy distribution and flux of electrons over the energy range from <1 eV to 20 keV, and of protons over the range from 50 eV to 60 keV. The overall flux levels in these ranges were expected to vary by more than six orders of magnitude. Cylindrical electrostatic deflection techniques were used as a basis for the spectrometer design. Detailed discussions of these instrumental techniques can be found in Roy and Carette[1], and in Servier.[2] The rather substantial range of energy and flux levels to be encountered presented problems that required a series of design compromises, or trade-offs, between mutually interdependent instrument parameters, all within the constraints of space appropriate to rocket payloads. The electron-proton spectrometer that ultimately

Received for publication 2 April 1982

1. Roy, D., and Carette, J. D. (1971) Electrostatic spectrometers, III, Can. J. Phys., 49:2138.

2. Servier, K. D. (1972) Low-Energy Electron Spectrometry, John Wiley, New York.

evolved was an integrated nesting of four analyzers in a single unit designed to measure electrons and protons over separate but overlapping energy ranges by means of incrementally stepped scans. Two electron-proton spectrometer units were planned for each of two Taurus-Orion rockets. The pair of units in each rocket were mounted to look in opposite directions to obtain more complete pitch-angle information. The overall experiment priorities were set as: (1) energy resolution relative to expected spectral structure, (2) altitude resolution, and (3) pitch-angle resolution.

2. INSTRUMENTATION

2.1 Electron-Proton Spectrometer Unit

Four identical units were mounted in the two rocket payloads. Figure 1 shows the basic configuration of each unit in schematic form. The four nested analyzers, I, IIA, IIB, and III are shown in cross section through their focusing planes.

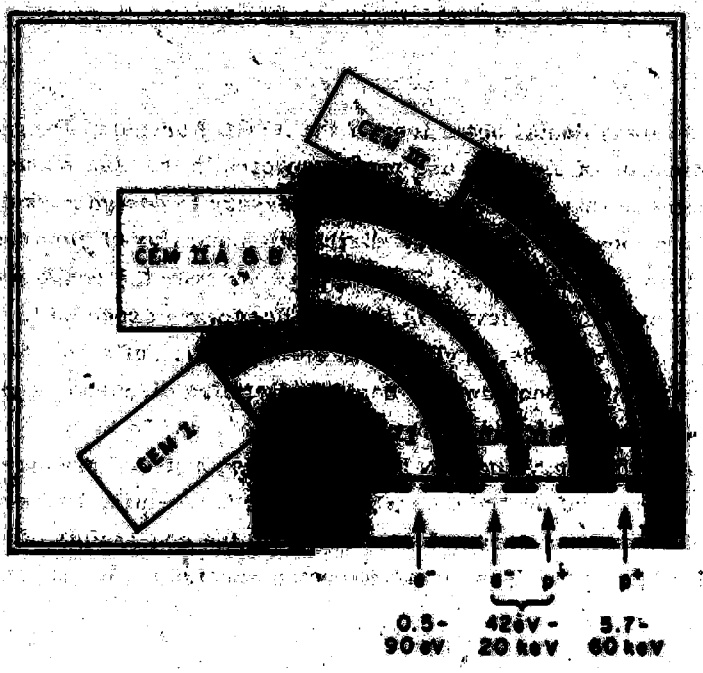

Figure 1. Schematic Representation of Electron-Proton Spectrometer Units, Shown in Cross-Section Through Their Focusing Planes. The units each consist of four separate analyzers, Channels I, IIA, IIB, and III, nested into a single assembly, and designed to measure the species shown over the energy ranges indicated. The detector elements are channel electron multipliers (CEM) mounted at the exit slits

Electrons (e^-), and protons (p^+), enter through the collimating apertures indicated. They then pass into the analyzer sections where they are deflected according to their energies by appropriate voltage differentials ΔV_A applied as $+1/2\ \Delta V_A$ to the curved deflector plates (shown in solid black). Finally, they are detected by the channel electron multipliers (CEM) mounted in Kel-F block assemblies at the exit slit of each analyzer. Analyzer Channel 1 is biased to measure electrons between 0.5 eV and 90 eV in 64 incremental steps; it has a deflection angle ϕ of 127° to achieve optimum focusing and energy resolution since the most marked spectral structure exists in this region. Analyzer Channels IIA and IIB share a common deflector plate (center), and are stepped simultaneously to measure electrons and protons in the energy range from 50 eV to 20 keV. A deflection angle $\phi = 90°$ was chosen for these analyzers as a compromise between conflicting requirements of instrument design. In this case, optimal focusing is not achieved, but both the geometric factors and energy bandwidths are increased, a necessity of low anticipated flux levels. The consequent degradation of resolution can be tolerated because no marked spectral structure was expected in this energy range. For similar reasons, ϕ is set at 60° for Energy Channel III, which is biased to measure protons between 5.7 and 60 keV in eight incremental steps. The three stepping sequences (IIA and IIB share a common stepped supply) are synchronized at the first step, and the dwell time per step for Analyzers II and III are, respectively, 2 and 8 times longer than for Analyzer I so that the total scan time for all is identical (1.28 sec/scan). This allows altitude resolution significantly less than 2 km/scan at worst, and less than 1 km/scan for the major portion of the flight. A summary of these and other relevant design parameters is given in Table 1.

Table 1. Electron-Proton Spectrometer Design Parameters

Analyzer Channel	I	IIA	IIB	III
Species	electrons	electrons	protons	protons
Energy range, E_o	0.5-90 eV	50 eV-20 keV	50 eV-20 keV	5.7-60 keV
Mean plate radius, $\bar{r}$	1.315 cm	2.310 cm	2.995 cm	3.982 cm
Plate separation, ΔP	0.528 cm	0.462 cm	0.599 cm	0.265 cm
Deflection angle, ϕ	127^o	90^o	90^o	60^o
Analyzer constant, $E_o/\Delta V_A$	1.244	2.5	2.5	7.52
Energy resolution, $\Delta E/E$	0.094	0.21	0.21	0.28
Stepping increment, $(E_n+1)/E_n$	1.08	1.22	1.22	1.44
No. steps/scan, n	64	32	32	8
Dwell time/step, Δt	20 msec	40 msec	40 msec	160 msec

2.2 Payload Configuration

Two electron-proton spectrometer units with support flight electronics were mounted on each of the two rockets. Launch was planned from Poker Flat Research Range, Alaska, along a trajectory of 030° true (000° magnetic). These vehicles were identified as 13.030 and 13.031. The mounting configuration for 13.031 is shown in Figure 2. The aperture axes of the EPS units were offset from the rocket longitudinal axis (R in the figure) by 38° for both the forward- and aft-looking units. The aspect angle of this rocket during the data-taking period was planned for 65°, and the roll rate was planned for 3 ±1 rpm. Thus, the aperture "look" axis would describe a cone during vehicle roll that at one limit would point it parallel to a line 13° due south (magnetic) of the zenith and, therefore, parallel to the geomagnetic vector B_E, the inclination at PFRR being 77° north. The total angle subtended by this look cone would then be 76°, as illustrated in Figure 2, so that the combined aft and forward instruments would sample magnetic pitch angles from 0° to 76°, and from 104° to 180°. At a 3-rpm roll rate this would sample magnetic pitch angles at 7.6°/sec or 9.73°/scan, a satisfactory pitch-angle resolution for this experiment. Rocket 13.030, considered primarily a back-up vehicle for this experiment, was constrained by requirements of another onboard experiment to maintain its longitudinal axis oriented toward the zenith, an aspect angle of 90°, during the data-taking period. In this case, the EPS aperture axes were offset 13° so as to include a zero pitch angle in its coning sample. This limited the look cones to magnetic pitch angles between 0° to 26° and 154° to 180°, resulting in a magnetic pitch-angle sampling rate of 2.6°/sec or 3.3°/scan at a 3-rpm roll rate.

Prior to launch, both forward and aft payload sections were enclosed in vacuum-tight compartments that allowed them to be purged by successive cycles of evacuation and dry nitrogen backfill while on the rails. On the upleg after launch, the nose cones and aft bulkheads were blown away, exposing the EPS apertures prior to the data-taking period.

2.3 Calibration

The 4 EPS units, 16 analyzer channels in all, were calibrated at the Rice University particle detector calibration facility. The calibration, an involved procedure, is performed, basically, to evaluate empirically the expression relating raw signal counts to absolute differential number flux j_n in units of $(cm^2\ sec\ sr\ eV)^{-1}$, where

$$j_n = \frac{\text{Raw sig}}{G_f\ \Delta t\ \eta\ \Delta E}$$

G_f is the geometric factor in cm^2 sr and is critically dependent on the physical dimensions of collimator and analyzer geometry; ΔE is the energy bandwidth, which is also highly dependent on physical analyzer parameters; and η is a factor less than unity that accounts for the effects of detector (CEM) efficiency, fringing fields, etc. Although the four instruments were identical in design, the fabrication and assembly of individual components to the highly precise tolerances required is difficult to achieve. For cylindrical deflection analyzers where $\phi \neq 127°$, moreover, there is no suitable method, at present, of calculating energy bandwidth ΔE accurately[3]. Added to this is the problem of potentially large variations in detector (channel electron multiplier) response efficiency to different particles and varying energies; therefore, a careful and precise calibration of each individual analyzer unit planned for flight on a spacecraft is of critical importance. A summary of the results of this calibration is shown in Table 2.

Table 2. Electron-Proton Spectrometer Calibration Data

	EPS-1 (031 Fwd)	EPS-2 (030 Fwd)	EPS-3 (030 AFT)	EPS-4 (031 AFT)
CHANNEL I				
Geometric Factor	2.92×10^{-4}	3.34×10^{-4}	3.88×10^{-4}	3.71×10^{-4}
Analyzer Constant	1.35	1.35	1.35	1.35
$\Delta E/E$	0.145	0.144	0.138	0.140
Solid Angle	$\alpha = 7.5°$	$\alpha = 9°$	$\alpha = 9°$	$\alpha = 8.5°$
	$\beta = 14°$	$\beta = 14°$	$\beta = 14°$	$\beta = 13°$
CHANNEL IIa				
Geometric Factor	1.25×10^{-3}	1.27×10^{-3}	1.39×10^{-3}	1.56×10^{-3}
Analyzer Constant	2.47	2.46	2.46	2.48
$\Delta E/E$	0.180	0.180	0.180	0.178
Solid Angle	$\alpha = 13°$	$\alpha = 12°$	$\alpha = 12°$	$\alpha = 12.5°$
	$\beta = 13.5°$	$\beta = 12°$	$\beta = 13°$	$\beta = 12°$
CHANNEL IIb				
Geometric Factor	8.03×10^{-4}	4.06×10^{-4}	5.45×10^{-4}	4.33×10^{-4}
Analyzer Constant	2.58	2.54	2.66	2.66
$\Delta E/E$	0.118	0.124	0.122	0.131
Solid Angle	$\alpha = 9.5°$	$\alpha = 12.0°$	$\alpha = 11.5°$	$\alpha = 11.5°$
	$\beta = 10°$	$\beta = 8.5°$	$\beta = 8.0°$	$\beta = 9.5°$
CHANNEL III				
Geometric Factor	1.10×10^{-3}	2.06×10^{-3}	1.87×10^{-3}	1.82×10^{-3}
Analyzer Constant	7.90	7.68	7.83	7.68
$\Delta E/E$	0.283	0.274	0.262	0.269
Solid Angle	$\alpha = 3.4°$	$\alpha = 7.7°$	$\alpha = 4.5°$	$\alpha = 5.8°$
	$\beta = 11.0°$	$\beta = 10.3°$	$\beta = 11.0°$	$\beta = 11.5°$

3. Arnow, M. (1976) Electrostatic cylindrical spectrometers, J. Phys. E: Sci. Instrum., 9:376.

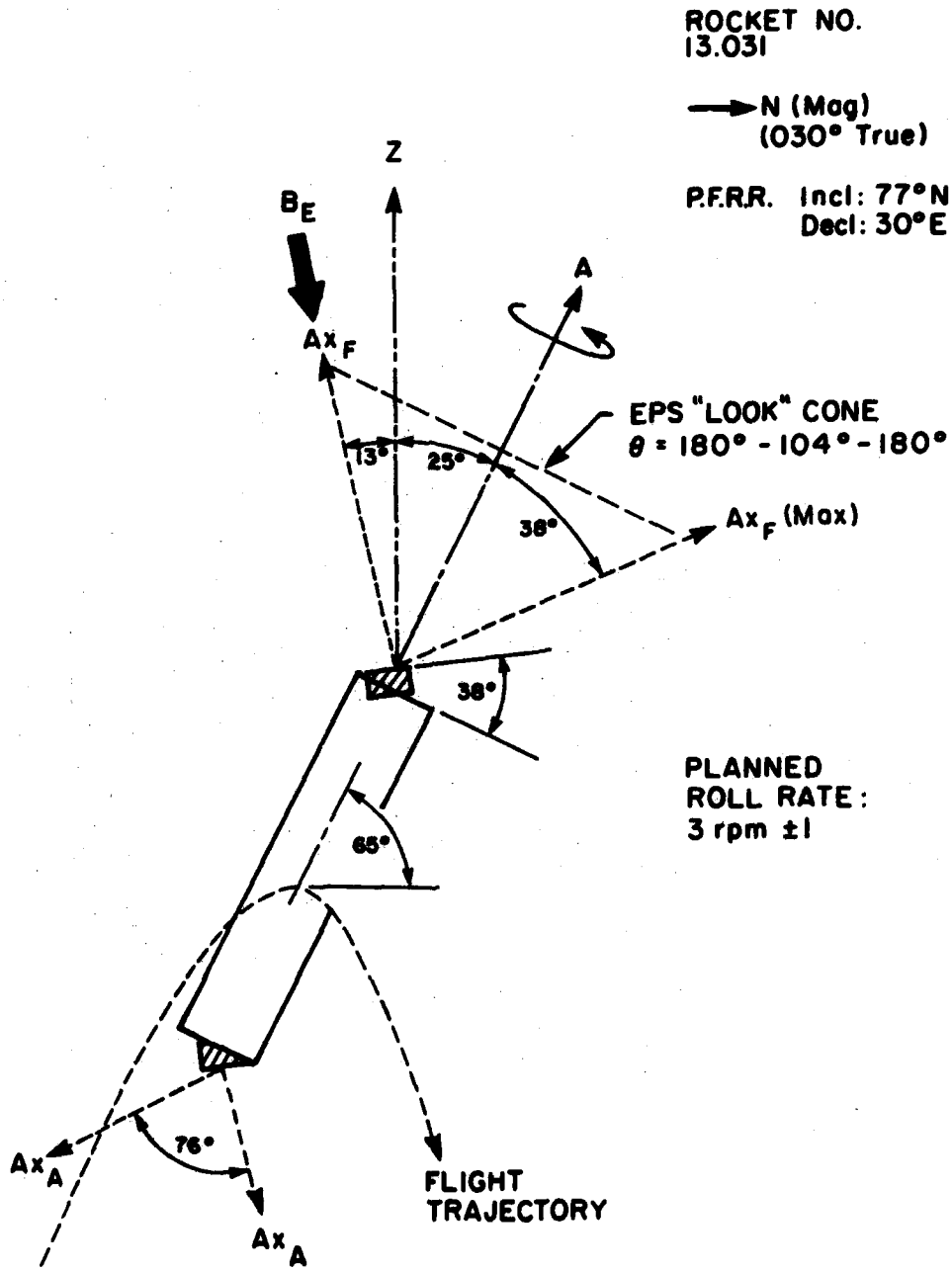

Figure 2. In-Flight Configuration of Rocket 13.301 and Payload. Vehicle aspect and roll were maintained by an on-board attitude control system. The trajectory ground path was due north (magnetic); the forward and aft electron-proton spectrometer (EPS) units were offset-mounted, as shown, so that their aperture axes Ax described a cone during vehicle roll. Each cone subtended a total angle of approximately 76°, aligned so that at one position each axis was parallel to the geomagnetic vector B_E, thus allowing the forward unit to sample pitch angles between 180° and 104°, and the aft unit between 0° and 76°

It is not surprising that in some cases there appear large deviations in the data of this table, in particular the geometric factor. Figures 3a through 3d are typical computer plots obtained during this calibration at the Rice University facility. These show relative signal in counts/sec on the vertical axis as a function of the angles α and β in the two orthogonal planes normal to the aperture plane, to illustrate typical instrument response near center energy for the four analyzer channels.

3. FLIGHT PERFORMANCE

The rockets were launched from Poker Flat Rocket Range into a diffuse aurora during the night of 6 March 1981. Rocket number 13.030 was launched at 2209.00 local time (0809 UT), reaching an apogee of 156.4 km; 13.031 was launched at 2226:00 LT, reaching an apogee of 169.7 km. Both rockets performed well. This

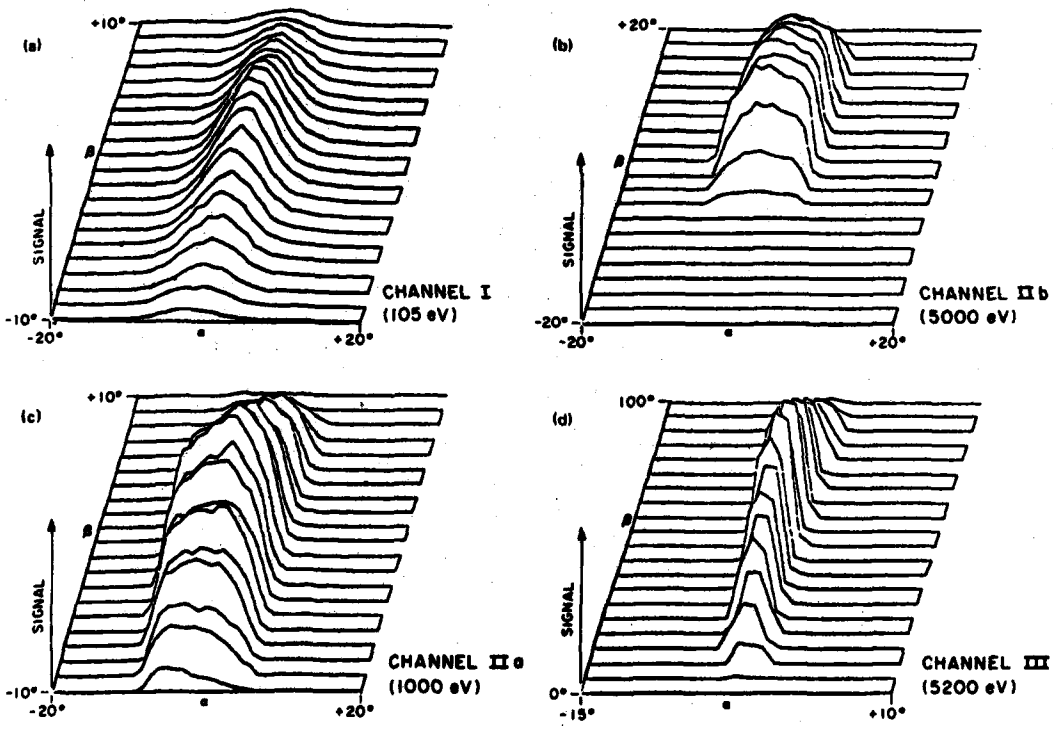

Figure 3a-d. Typical Calibration Curves for Each of the Four Analyzer Channels in an Electron-Proton Spectrometer Unit. These computer plots show relative signal in counts/second on the vertical axis as a function of α and β in the two orthogonal planes normal to the aperture plane, illustrating analyzer angular response near center energy

is illustrated in Figure 4, which shows pitch angle (and altitude) as a function of time after launch for 13.031. The aspect angle and roll rate were well established before the EPS units were turned on (97 seconds into the flight), and were maintained closely during the data-acquisition period. The plot shows a roll rate of almost exactly 3 rpm, and a pitch-angle sampling segment of about 75°, which is very close to the planned performance.

Useful data were returned from all four channels on three of the four payloads throughout the flights. The forward section on 13.030 experienced an electronics failure during the upleg and returned only partial data. Examination of the analog housekeeping records later stripped from the telemetry tape indicate that this was due to the failure of a 40 V power supply on this payload.

4. PRELIMINARY DATA

At this writing, the flight data have not been reduced completely. The most fully evaluated data to date have been those of the lower energy electrons. It is here that the most marked spectral structure is present. Immediately noteworthy in these data was clear evidence that both vehicles had acquired a very low level of skin charge V_s during flight, less than 0.5 V, as compared with the 1-2 V skin-charge levels normally encountered in daytime midlatitude flights. This will be discussed further in a later paragraph. Figure 5 is a three-dimensional computer

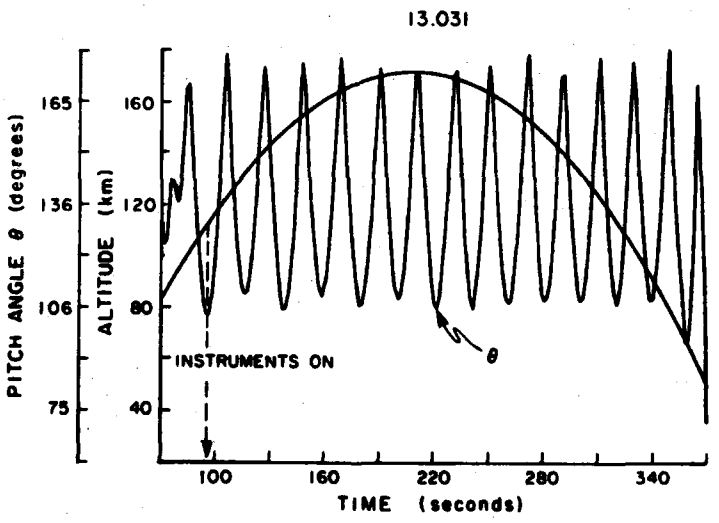

Figure 4. Pitch Angle and Altitude as a Function of Time After Launch for Rocket 13.031. The point at which the EPS units were turned on in this flight is indicated

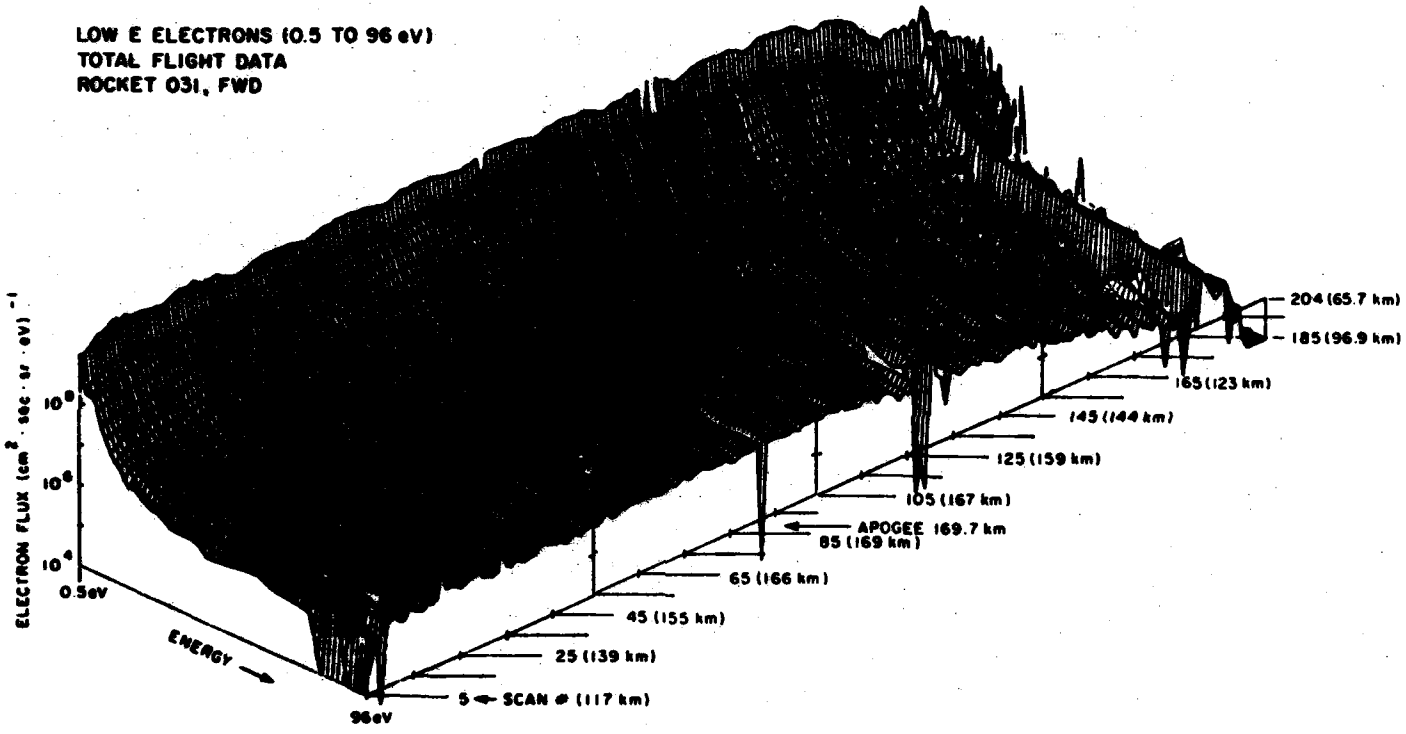

Figure 5. Computer Plot Showing Typical Individual Energy Spectra Over the Entire Flight for the Low-Energy Electron Analyzer (Channel I) of One Electron-Proton Spectrometer Unit. Signal, on the vertical axis, as a function of energy on the conventional x axis, is shown for each consecutive scan, numbered along the third axis along with corresponding altitudes. The occasional sharp excursions are due to electronic transients and can be ignored

plot representing individual energy spectra obtained from Energy Channel I for the entire flight of the forward-looking instrument on 13.031. Electron differential number fluxes over some four orders of magnitude are shown on the vertical axis versus energy between 0.5 and 96 eV plotted on the conventional x axis. Shown along the third axis are the 204 individual spectral scans obtained during the 261 sec data-acquisition period of this flight; these are marked off in 10 scan intervals along this axis, with corresponding altitudes shown in parentheses at every 20th scan. The lower numbered scans represent upleg data, apogee was reached at scan numbers 87-88, and the remaining scans are downleg data. The deep excursions seen around scan numbers 5, 90, and 126 are due to short-lived electronic transients; these were seen in the data from all energy channels of this instrument simultaneously, and can be ignored.

Typical individual spectra at various altitudes for this analyzer channel can be seen more clearly in the two-dimensional computer plot of Figure 6a. For comparison, Figure 6b shows equivalent spectra obtained from the downward looking instrument on 13.030. There do not appear to be any large differences in flux values, or in the overall structure, between forward- and aft-looking analyzers in these data, which were obtained from two different rockets flown 17 min apart. The spectra obtained from the remaining low-energy channels, 13.030 forward and 13.031 aft, were essentially identical to the foregoing, as shown in Figures 6c and 6d. The data in Figure 6c were limited to upleg measurements, due to the flight electronics failure in the 13.030 forward payload mentioned previously. All of these spectra show the plateau or valley-like structure around 2.5 eV, which is attributed to energy loss caused by resonant vibrational excitation of N_2. Although the 2-5 eV region to which this spectral feature is confined represents a very small part (<0.02 percent) of the total electron energy range of concern in this experimental program, the spectra here are of sufficient importance to merit further discussion. Data relating to this region, therefore, are presented in more detail in the Appendix.

The higher energy electron data from the IIA channels have been less fully reduced. Figure 7 shows typical spectra up to 4 keV obtained from all three experimental payloads that returned data. These spectra, taken at the two common altitudes shown, indicate that the 1 keV flux levels measured by the forward-looking instrument (downcoming electrons) were a factor of 2 to 3 greater than the aft-looking analyzer on the same rocket, 13.031. The forward payload on 13.030, as mentioned earlier, failed early in flight, but data from the aft instrument on this rocket agree very closely at common altitude with those obtained by the aft counterpart on 13.031 flown 17 minutes later. There was a 50 eV overlap in the energy ranges covered by the two analyzer channels I and IIA (from 40 to 90 eV) that allowed a quantitative comparison of the electron flux levels simultaneously

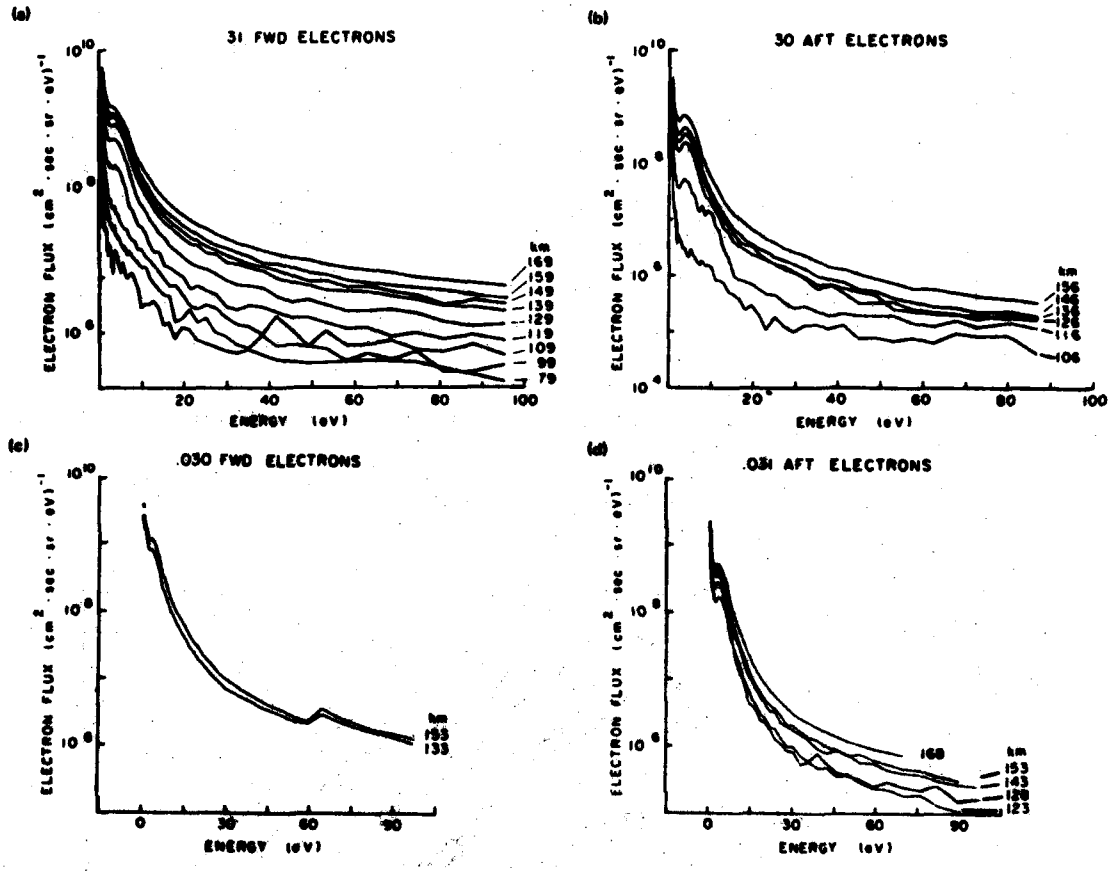

Figure 6a-d. Energy Spectra Obtained From the Four Low-Energy Electron Channels at Various Altitudes. Only partial data was obtained from 13.030 Fwd. (Fig. 6c) due to an electronics failure in that payload section

measured by each and, thereby, an inflight quasi calibration. An example of this is included in Figure 7 where the small solid circles show data points from both of the Channel I analyzers on 13.031 corresponding to the simultaneously obtained data from both IIA analyzers on this rocket at apogee. As shown, the quantitative agreement in the overlap range is well within statistical limits, and supports a reasonably good confidence factor for the data within this energy region.

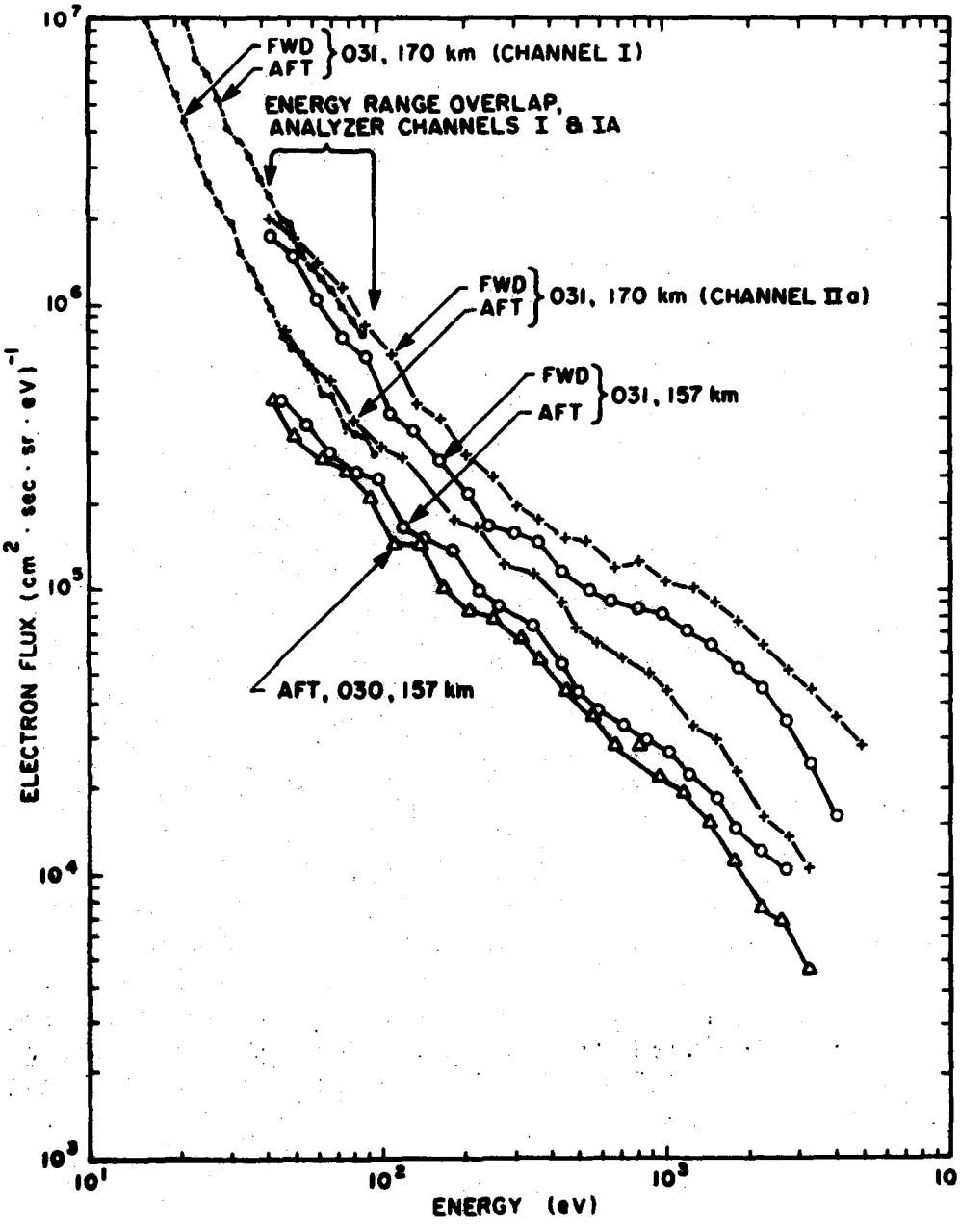

Figure 7. Energy Spectra to 4 keV Obtained From Channel IIA of the Three Working Electron-Proton Spectrometer Units. Also shown are simultaneously obtained data from Channel I of both 13.031 units to illustrate the quantitative agreement between these energy channels

References

1. Roy, D., and Carette, J. D. (1971) Electrostatic spectrometers, III, Can. J. Phys., 49:2138.

2. Servier, K. D. (1972) Low-Energy Electron Spectrometry, John Wiley, New York.

3. Arnow, M. (1976) Electrostatic cylindrical spectrometers, J. Phys. E: Sci. Instrum., 9:376.

4. McMahon, W. J., and Heroux, L. (1978) Rocket measurement of thermospheric photoelectron energy spectra, J. Geophys. Res., 83:1390.

5. Doering, J. P., Peterson, W. K., Bostrom, C. O., and Potemra, T. A. (1976) High resolution daytime photoelectron energy spectra from AE-E, Geophys. Res. Lett., 3:129.

6. Lee, J. S., Doering, J. P., Potemra, T. A., and Brace, L. H. (1980) Measurements of the ambient photoelectron spectrum from Atmospheric Explorer: I. AE-E measurements below 300 km during solar minimum conditions, Planet. Space Sci., 28:947.

7. Ashihara, O., and Takayangi, K. (1974) Velocity distribution of ionospheric low-energy electrons, Planet. Space Sci., 22:1201.

8. Mantas, G. P., and Bowhill, S. A. (1975) Calculated photoelectron pitch angle and energy spectra, Planet. Space Sci., 23:355.

9. Jasperse, J. R. (1977) Electron distribution function and ion concentration in the earth's lower ionosphere from Boltzmann-Fokker-Planck theory, Planet. Space Sci., 25:743.

Appendix A

The 2-5 eV Region of Electron Energy Spectra

The plateau or valley-like structure due to N_2 vibrational losses appears in all spectra shown in Figures 6a through 6d. This structural feature has been seen previously in rocket measurements of midlatitude daytime thermospheric photoelectrons,[4] and by satellite instruments.[5,6] The observed prominence of this structure, that is, the depth of the valley at about 2.5 eV with respect to the peak at about 4 eV, has, in all cases, been less than that generally predicted by theory.[7-9] In the present experiment, this valley is even less prominent than the valley observed by essentially identical instrumentation used for the rocket

4. McMahon, W. J., and Heroux, L. (1978) Rocket measurement of thermospheric photoelectron energy spectra, J. Geophys. Res., 83:1390.
5. Doering, J. P., Peterson, W. K., Bostrom, C. O., and Potemra, T. A. (1976) High resolution daytime photoelectron energy spectra from AE-E, Geophys. Res. Lett., 3:129.
6. Lee, J. S., Doering, J. P., Potemra, T. A., and Brace, L. H. (1980) Measurements of the ambient photoelectron spectrum from Atmospheric Explorer: I. AE-E measurements below 300 km during solar minimum conditions, Planet. Space Sci., 28:947.
7. Ashihara, O., and Takayangi, K. (1974) Velocity distribution of ionospheric low-energy electrons, Planet. Space Sci., 22:1201.
8. Mantas, G. P., and Bowhill, S. A. (1975) Calculated photoelectron pitch angle and energy spectra, Planet. Space Sci., 23:355.
9. Jasperse, J. R. (1977) Electron distribution function and ion concentration in the earth's lower ionosphere from Boltzmann-Fokker-Planck Theory, Planet. Space Sci., 25:743.

measurements of thermospheric photoelectrons. Defining a peak-to-valley ratio as a simple index of this structural prominence for comparative purposes, the ratios obtained in the present nighttime auroral spectra appear to be significantly less, in all cases, than those observed in the daytime thermospheric photoelectron data. This is illustrated in Figure A1, which shows the ratios obtained from both experimental series. In addition, the auroral electron ratios obtained from the upward-looking analyzers were, for both instruments, much lower than those from their two aft-looking counterparts. As shown in Figures 6a and 6c, the spectral structures from both forward analyzers represent near-plateaus at their maximum prominence, in contrast to the shallow but clearly defined valleys measured by both aft-looking instruments. The former data resulted in ratios so close to unity

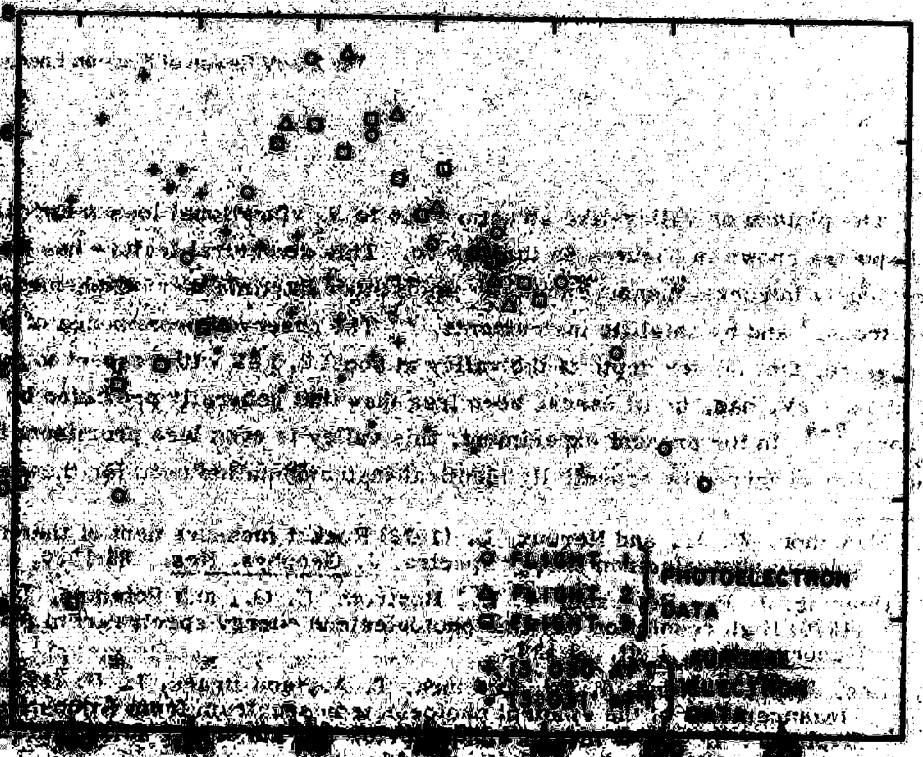

that they did not merit plotting on Figure A1. Another significant discrepancy between measurement and generally accepted theory has been an observed reversal and decline in the prominence of this structure in the thermospheric photoelectron spectra as altitude decreased below about 140 km. This is illustrated in the photoelectron data of Figure A1, and is in contrast to theoretical predictions that the feature should continue to increase in prominence as altitude decreases below this 140 km region. As also shown in Figure A1, however, no such reversal appears indicated in the auroral electron data from both aft-looking instruments down to about 110 km. The much weaker prominence of this structure found in the data from the upward-looking instruments does not allow discernment of any trend as a function of altitude.

Profiles of fixed-energy flux values versus altitude at several representative energies are shown, with pitch angle θ data superimposed, in Figure A2. There are observable oscillations in some of these flux value curves. The oscillations are most prominent at the lower energies. A direct relationship between pitch-angle cycling and the low-energy flux variations is apparent. An analysis of electron trajectories that, as a function of pitch angle, should fall within the acceptance cone of the analyzer aperture for this payload/vehicle configuration, rules

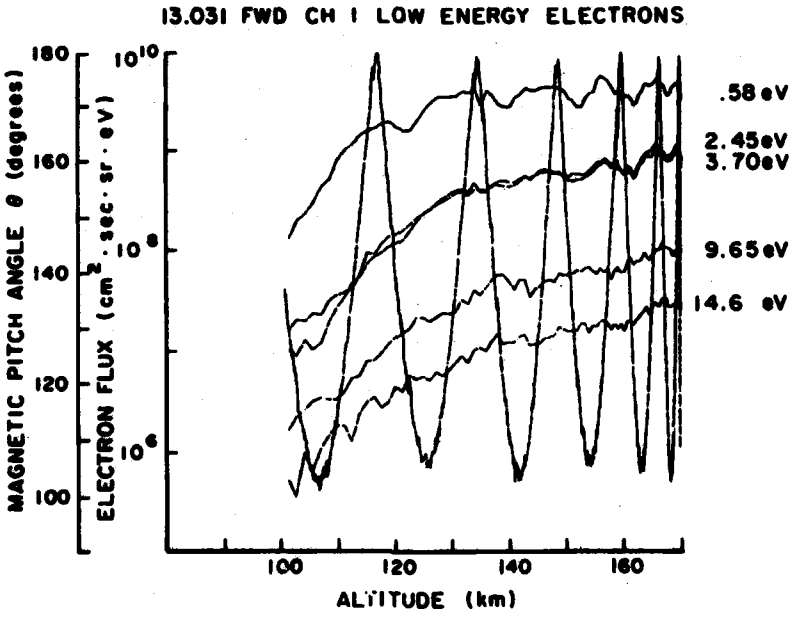

Figure A2. Constant Channel I Energy Profiles at Several Fixed Values, Along With Corresponding Pitch-Angle Values, as a Function of Altitude. The flux oscillations at the lower fixed energies are discussed in the text

out geomagnetic shadowing as a cause of this behavior. For 1 eV electrons, the onset of such shadowing would not occur until a pitch-angle differential $\Delta\theta > 75^\circ$ was reached ($\theta = 105^\circ$ in Figure A2); for higher energies, greater $\Delta\theta$s could be tolerated, a condition not encountered on this flight.

These cyclic lower energy flux variations were almost certainly due to the effects of geomagnetic field penetration into the deflection chamber of the analyzer. One of the compromises required in the mechanical design of this payload was the necessity, for practical engineering reasons, of omitting mu-metal shielding around the analyzers. It was known that this would have virtually no impact on energies above about 10 eV in a total experimental range extending to 20 keV for electrons. Balanced against the additional cost and complications that the addition of effective mu-metal shielding would impose on the fabrication and assembly of these prototype instruments under the time constraints that were involved, this omission was considered necessary. The pitch-angle sampling was a requirement of the higher energy measurements, and was simply to be tolerated by the low-energy experiment because isotropy was expected throughout the altitude range of these measurements. The effect, then, on the very low energy signal resulting from the absence of shielding became the observable function of pitch angle variations shown in Figure A2. This makes it possible to assess, to a degree, the extent of data degradation that resulted, and to support a conclusion that the spectral shape of the 2-5 eV structure was not, in relative terms, significantly changed as a result. In fact, these spectra can be viewed as about qualitatively equal to the corresponding photoelectron spectra for the following reason: Even where effective shielding is present, as was the case for all the thermospheric photoelectron measurements, the determination of absolute flux values in this low-energy region is normally very difficult because of the effects of vehicle skin charge V_s. Corrections must be made for this, and are accurate only to the extent to which V_s can be determined accurately. V_s values encountered in the midlatitude daytime photoelectron flights were consistently in the 1-2 V range, as determined by the difference between measured and known energies associated with established processes that produce spectral structure. Skin charge can usually be determined to an accuracy of $\pm$ 0.5 V for this instrumentation. Corrections for an estimated V_s = 1.5 V in this accuracy range result in quantitative uncertainties of nearly $\pm$ 40 percent in the absolute flux of 3 eV electrons.[4] Although this uncertainty declines very rapidly as energy increases, it is substantial in the 0-3 eV spectral region. In the present experiment, however, V_s levels of less than 0.5 V were encountered during both flights, greatly reducing the attendant quantitative uncertainties. The absence of magnetic shielding, in this case, produced uncertainties of an equal magnitude at this energy level. The fixed energy profiles at 2.4 and 3.7 eV in Figure A2 indicate flux variations of

about ± 30 percent from a median value, and their departure from a true value in absolute terms cannot be assessed accurately. These two energies approximately represent the valley and peak points, respectively, although for these particular data the shape is more that of a plateau, so that one profile curve virtually replicates the other. This replication serves to illustrate more clearly the synchronous nature of these flux variations, which provides evidence that the shape of this structure in the 2-5 eV region is, in relative terms, depicted with reasonable accuracy in the energy spectra of Figure 6a through 6d. The near congruence of these fixed-energy data point curves is to be expected from the fact that, within a given energy scan, these points on the spectra were sampled for 20 msec periods, 100 msec apart. The roll rate of this vehicle resulted in a pitch-angle sampling rate of about 7.5°/sec, which represents a pitch-angle difference of < 1° between these major points in the structure. Figure A2 also shows, as expected, that the flux variations of the constant energy profiles decrease as energy increases, and that at the 14.6 eV point these are indiscernible in the statistical fluctuations.